Application and Validation of Regression Analysis in the Prediction of Discharge in Asymmetric Compound Channels

Issam A. Al-Khatib[1]; Hassan Abu Hassan[2]; and Khaled A. Abaza[3]

Abstract: A series of laboratory experiments was performed to present the overbank flow in asymmetric rectangular compound channels. For this purpose, two different sets of asymmetric models with rectangular compound cross sections were tested for a wide range of discharges. The first set consisted of nine compound cross-section models formed by a combination of three step heights and three main channel widths. The second set consisted of six compound cross section-models formed using a combination of two step heights and three main channel widths. The mean flow measurements were then related to a dimensionless parameter called the relative depth defined as the ratio of the depth above the floodplain bed to the depth above the main channel bed. The variations and interactions of the three outlined mean flows were investigated with respect to relative depth. A set of single-variable regression models has been developed for estimating the three mean flow types using relative depth as the only independent variable. Another set of multiple-variable regression models was derived using two additional dimensionless parameters, which take into account the width dimensions of the constructed asymmetric compound channel. The application of several key statistics and validation procedures indicated the high significance and reliability of the developed models in predicting the three mean flow types. **DOI: 10.1061/(ASCE)IR.1943-4774.0000579.**

CE Database subject headings: Regression analysis; Open channel flow; Experimentation; Predictions; Water discharge; Validation.

Author keywords: Flow distribution; Compound channel; Regression analysis; Open-channel flow.

Introduction

River flows require careful management for power generation, flood alleviation, and water supply as well as amenity uses, and they are often affected by human activities. River management and design has tended to be dominated by engineering concerns. River design is becoming more environmentally sensitive, seeking solutions that are sustainable and ensuring flood protection. A flood alleviation solution that offers environmental advantages is that of a two-stage or compound river geometry consisting of a deep central main channel flanked by one or two floodplains. Such cross sections ensure reasonable depths at low flows, whereas the floodplains increase conveyance during high flows. The floodplain areas are, however, often developed for housing purposes, agricultural, or commercial uses, which raises the issue of flood risk and flood protection (Myers et al. 2000).

Understanding the hydraulic behavior of compound channels consisting of a main channel and floodplains is necessary for the design of economical flood protection schemes and for accurate prediction of river flood levels. Normally, laboratory studies are conducted to provide much of the knowledge about the effects of overbank flows on sediment dynamics and discharge because it is difficult to obtain sufficiently accurate and comprehensive field measurements in natural rivers under unsteady flood flow conditions (Atabay et al. 2005). That is why practitioners are always searching for suitable means of estimating mean velocity and discharge in a variety of channel shapes and sizes (Maghrebi and Ball 2006).

Compound channels have received considerable attention over the past three decades because of their relevance in flood studies and in understanding river morphology (Knight and Demetriou 1983; Knight and Hamed 1984; Anderson et al. 1996; Knight et al. 1999; Ervine et al. 2000; Knight and Brown 2001; Babaeyan-Koopai et al. 2002; Carollo et al. 2002). In compound channels, even if the main channel and floodplains have the same roughness, the use of an overall hydraulic radius as a parameter to characterize the geometric properties of the section does not lead to good results for calculating mean velocity and discharge by standard equations such as the Manning's equation. The failure of this traditional method is attributable to the presence of a momentum transfer mechanism between floodplains and the fast-flowing main channel, which is characterized by lower velocities and depths (Bousmar et al. 2004; Rezaei and Knight 2011). This momentum transfer causes increases in velocity and discharge in floodplains, together with reductions in the corresponding main channel parameters (Hosseini 2004).

The estimation of flow rate corresponding to a certain depth is a common task for hydraulic engineers, and the accurate prediction of discharge for overbank stage is very important because this issue is directly related to flood-risk mitigation. Although the procedure for the estimation of the stage-discharge relationship for in-bank flows is conventional, it becomes more difficult when flow goes overbank. The accuracy of the estimations of overbank

[1]Associate Professor, Institute of Environmental and Water Studies, Birzeit Univ., P.O. Box 14, Birzeit, West Bank, Palestine (corresponding author). E-mail: ikhatib@birzeit.edu; ikhatib2012@yahoo.com

[2]Assistant Professor, Head, Applied Statistics Master Program, Birzeit Univ., P.O. Box 14, Birzeit, West Bank, Palestine.

[3]Professor, Dept. of Civil Engineering, Birzeit Univ., P.O. Box 14, Birzeit, West Bank, Palestine.

Note. This manuscript was submitted on July 1, 2012; approved on January 14, 2013; published online on January 16, 2013. Discussion period open until December 1, 2013; separate discussions must be submitted for individual papers. This paper is part of the ***Journal of Irrigation and Drainage Engineering***, Vol. 139, No. 7, July 1, 2013. © ASCE, ISSN 0733-9437/2013/7-542-550/$25.00.

stage-discharge curves and the subsequent assessments of low, moderate, and significant floodplain flood risk affect the drawing up of property insurance premiums, floodplain property values, planning requirements, flood risk maps, infrastructure location, and floodplain land use (Wormleaton et al. 1982; Ackers 1992, 1993; Lambert and Myers 1998; Shiono et al. 1999; Myers et al. 1999; Karamisheva et al. 2005, 2006).

The primary objective of this research is to introduce general equations, which can be applied to component discharges in asymmetric compound channels with homogeneous roughness to find more accurate values of the main channel and floodplain discharge values. The dependency of these general equations on dimensionless geometric parameters of the channel is also demonstrated.

Setup and Experiments

The first set of tested models consisted of nine different asymmetrical rectangular compound cross sections constructed using three different step heights and three different main channel widths. A rectangular glass-walled laboratory flume of 7.5 m long, 0.30 m wide, and 0.3 m deep with 0.0025 bottom slope was constructed in the fluid mechanics laboratory, Mechanical Engineering Department, Birzeit University, Palestine, and used to conduct the relevant experiments. The discharge was measured volumetrically with a digital flow meter that reads the rate directly (instantaneously) in m^3/h with 0.1 L accuracy. A point gauge was used along the centerline of the flume for head measurements. All depth measurements were done with respect to the bottom of the flume. A pitot tube of circular section with external diameter of 8 mm was used to measure the static and total pressures, which were then deployed in computing the velocities at specified points located along the nine compound cross sections used in the experiments conducted throughout this study.

The prototype models of asymmetric rectangular compound cross sections were fabricated from Plexiglas and placed at approximately the midlength of the laboratory flume. Fig. 1 shows the plan view and cross section of the models with symbols designating the significant dimensions of the model elements. The first set of prototype models were constructed using a 30 cm flume width (B_O) with specific width dimensions defining the nine distinct compound cross sections (Table 1). The symbols (B) and (Z) represent the width and step height of the main channel of the asymmetric compound cross section, respectively.

The required experiments were first conducted using the models with the smallest main channel width ($B = 10$ cm) while varying the main channel step height ($Z = 2$, 4, and 6 cm). Then, the main channel width (B) was increased to 15 cm with the step height (Z) taken on the same three values as before, and finally B was increased to 20 cm with the same three values of Z. This results in a total of nine distinct models with different values of B and Z. The width of the entire compound cross section (B_O) was maintained constant at 30 cm for all nine tested models. Therefore, the values for the floodplain width (B_f) as provided in Table 1

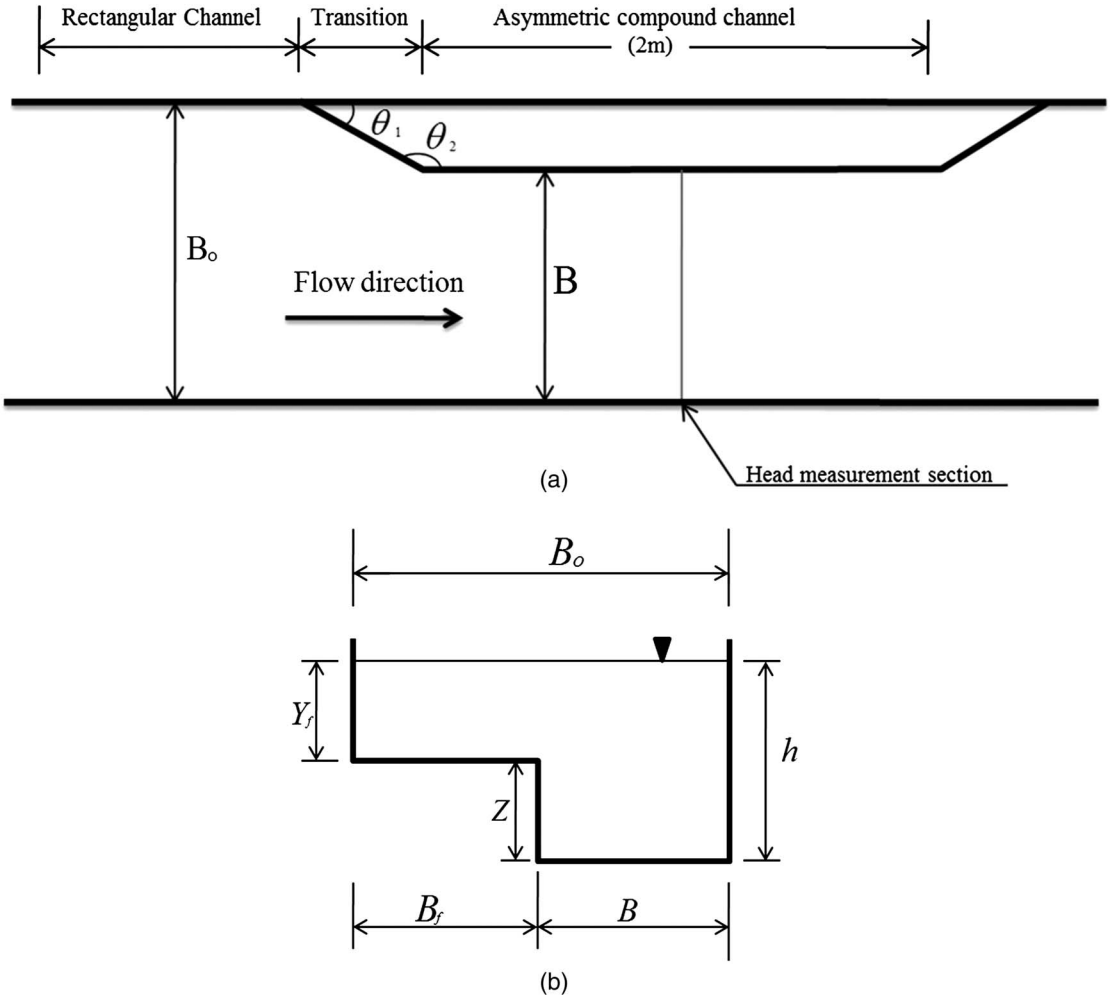

Fig. 1. Definition sketch of the flume used in the experiments: (a) plan view; (b) cross section of the asymmetric rectangular compound channel

J. Irrig. Drain Eng. 2013.139:542-550.

Table 1. Geometrical Properties of the Asymmetric Compound Channel Models for 30-cm Flume Width (B_O)

Compound cross section type (j)	B (cm)	Z (cm)	B_f (cm)	B_O (cm)	B_O/B_f	B_O/Z	B_O/B	B_f/Z	B_f/B	B/Z
1	10	2	20	30	1.50	15.00	3.00	10.00	2.00	5.00
2	10	4	20	30	1.50	7.50	3.00	5.00	2.00	2.50
3	10	6	20	30	1.50	5.00	3.00	3.33	2.00	1.67
4	15	2	15	30	2.00	15.00	2.00	7.50	1.00	7.5
5	15	4	15	30	2.00	7.50	2.00	3.75	1.00	3.75
6	15	6	15	30	2.00	5.00	2.00	2.50	1.00	2.5
7	20	2	10	30	3.00	15.00	1.50	5.00	0.50	10.00
8	20	4	10	30	3.00	7.50	1.50	2.50	0.50	5.00
9	20	6	10	30	3.00	5.00	1.50	1.67	0.50	3.33

Table 2. Geometrical Properties of the Asymmetric Compound Channel Models for 60-cm Flume Width (B_O)

Compound cross section type	B (cm)	Z (cm)	B_f (cm)	B_O (cm)	B_O/B_f	B_O/Z	B_O/B	B_f/Z	B_f/B	B/Z
10	15	3	45	60	1.3	20	4.0	15	3.0	5.0
11	15	6	45	60	1.3	10	4.0	7.5	3.0	2.5
12	20	3	40	60	1.5	20	3.0	13.3	2.0	6.7
13	20	6	40	60	1.5	10	3.0	6.7	2.0	3.3
14	25	3	35	60	1.7	20	2.4	11.7	1.4	8.3
15	25	6	35	60	1.7	10	2.4	5.8	1.4	4.2

were determined to be 20 cm for the first three models, 15 cm for the second three models, and 10 cm for the last three models. The transition length was selected to be twice the floodplain width (B_f). The entrance angles, θ_1 and θ_2, were specified to be equal to 26.565 and 153.35 degrees, respectively; and the length of asymmetrical rectangular compound channel section in all tested models was 2 m [Fig. 1(a)].

A second set of prototype models of asymmetrical rectangular compound cross sections were also fabricated from Plexiglas but using 60 cm flume width and 12 m length. The second set of models includes six additional cross-section types, numbered 10–15, as provided in Table 2. The specific width dimensions and dimensionless parameters associated with model types 10–15 are provided in Table 2.

For the purpose of determining the velocity distribution in the rectangular compound cross sections, the channel cross section was divided into a number of successive small sections normal to the direction of flow. Then, the total and static heads were measured at several points along the lines separating those small sections from each other by the use of pitot (Preston) tube. More points were taken close to the channel boundary. In addition, more velocity measurements were taken, especially at the intersection of the main and floodplain channels in an effort to capture the momentum interaction between the main channel and floodplain. Fig. 2 shows a definition sketch for the vertical lines over which the velocity measurements were made in the nine tested models. Fig. 2 shows the spacing of the vertical lines at the intersection of the main and floodplain channels is selected to be 1 cm. For the models with step size $Z = 2$ cm, the 8 mm pitot probe was used to take five velocity measurements at 4, 8, 12, 16, and 20 mm of the main channel vertical dimension. However, toward the free surface, the distance between the selected points along the vertical lines was increased.

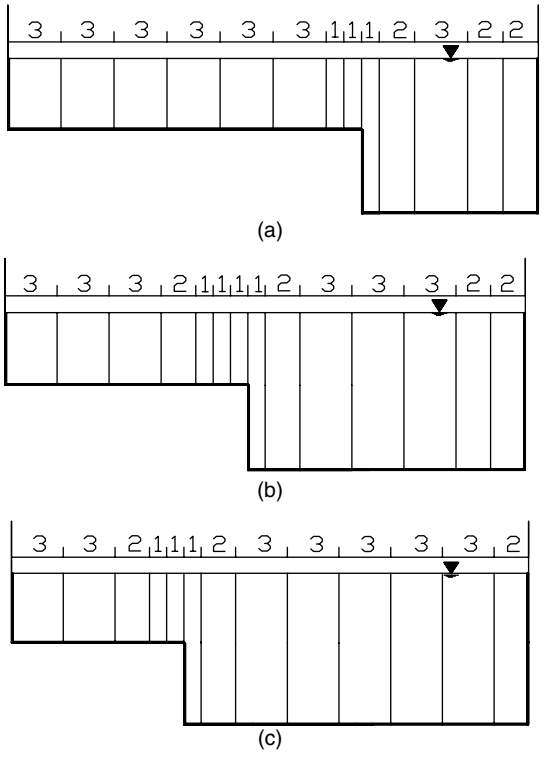

Fig. 2. Definition sketch for vertical lines over which velocity measurements were made for the different models (dimensions are in cm): (a) asymmetric compound cross-section Types 1, 2, and 3; (b) asymmetric compound cross-section Types 4, 5, and 6; (c) asymmetric compound cross-section Types 7, 8, and 9

Presentation and Discussion of Results

This section presents the experimental data pertaining to the three measured mean volumetric flow rates associated with the main channel, floodplain bed, and total compound channel, and it investigates their relationship with respect to the relative depth. It also provides the single-variable regression models predicting the three mean volumetric flow rates as a function of relative depth. Finally, the multiple-variable regression models are presented using three independent variables that include relative depth and

J. Irrig. Drain Eng. 2013.139:542-550.

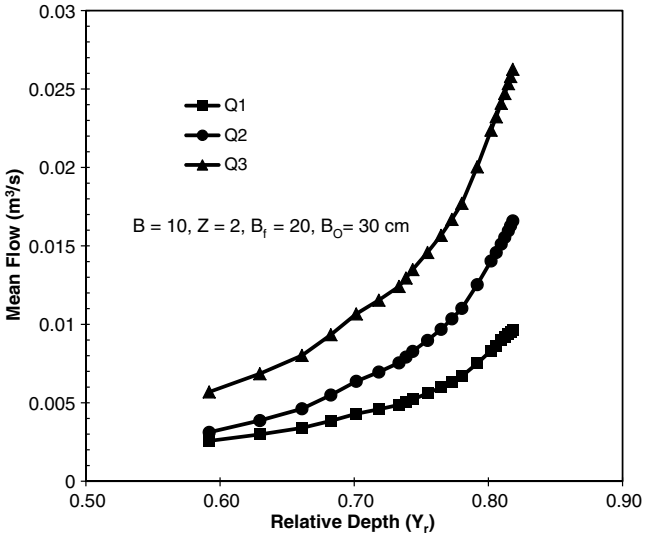

Fig. 3. Mean flow data for compound cross-section Type 1

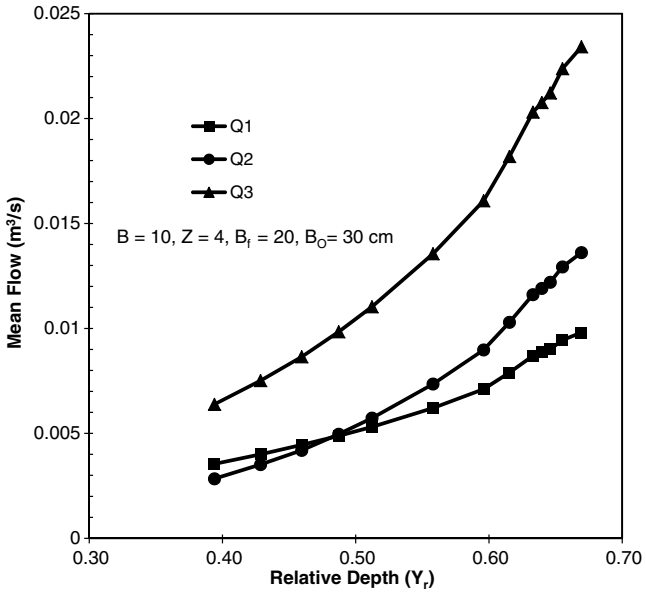

Fig. 4. Mean flow data for compound cross-section Type 2

two additional dimensionless parameters, which are function of the channel width dimensions and step height.

Variation of Mean Flow Distribution with Relative Depth

Mean volumetric flow-rate distribution in the main channel, floodplain, and total asymmetrical compound section was obtained for different depths of volumetric flow rate (h). All these depths were within the full compound cross-section depth as defined by the specific geometry of each model. The following notations are used to define the three different types of mean volumetric flow rates that are obtained from the measurements at the corresponding cross sections: Q_1 = mean volumetric flow rate in the main channel; Q_2 = mean volumetric flow rate in the floodplain; and Q_3 = mean volumetric flow rate in the total asymmetric compound cross section. In this study, the numerical integration has been used for the calculation of the three mean volumetric flow rates (Q_1, Q_2, and Q_3) as defined in the following:

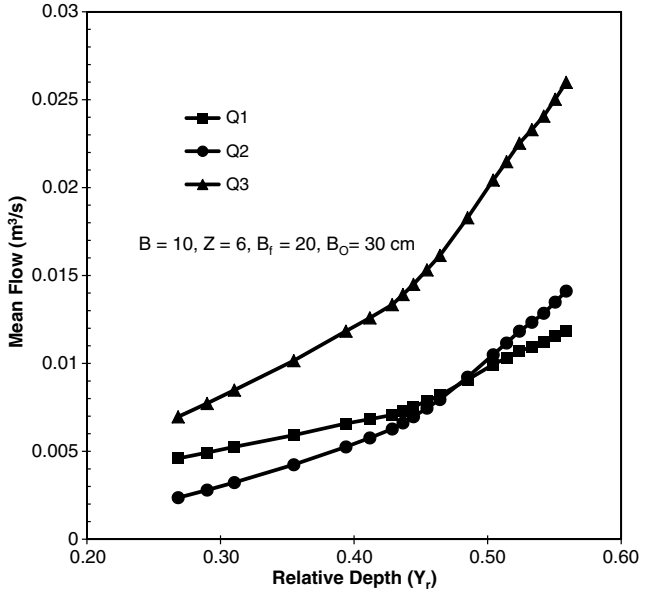

Fig. 5. Mean flow data for compound cross-section Type 3

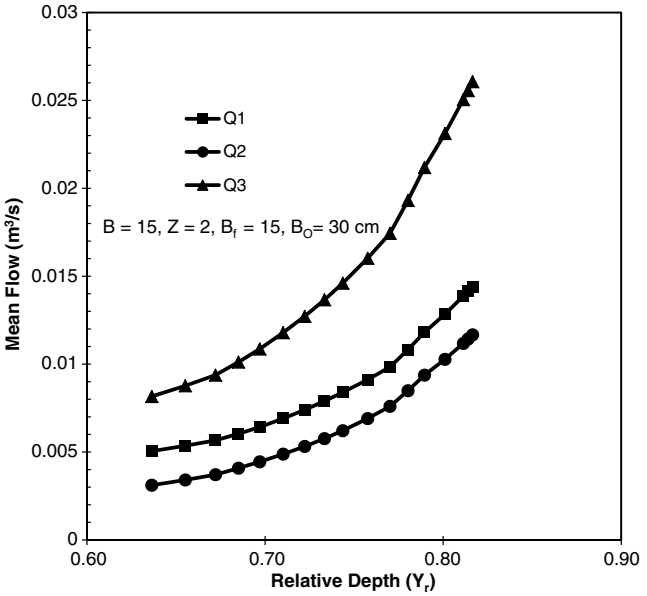

Fig. 6. Mean flow data for compound cross-section Type 4

$$Q = \int_A u_i dA_i \tag{1}$$

The cross sectional flow area (A) of the channel was divided into (N) number of differential areas (ΔA_i); and for each area, the corresponding average velocity (u_i) was determined from the measured velocities. The cross-sectional mean volumetric flow rate (Q) was calculated using Eq. (2), which provides a good approximation of Eq. (1).

$$Q \cong \sum_{i=1}^{N} u_i \Delta A_i \tag{2}$$

The aforementioned three mean volumetric flow-rate types have been plotted against the relative depth parameter (Y_r) for each of the nine manufactured compound rectangular cross sections with

J. Irrig. Drain Eng. 2013.139:542-550.

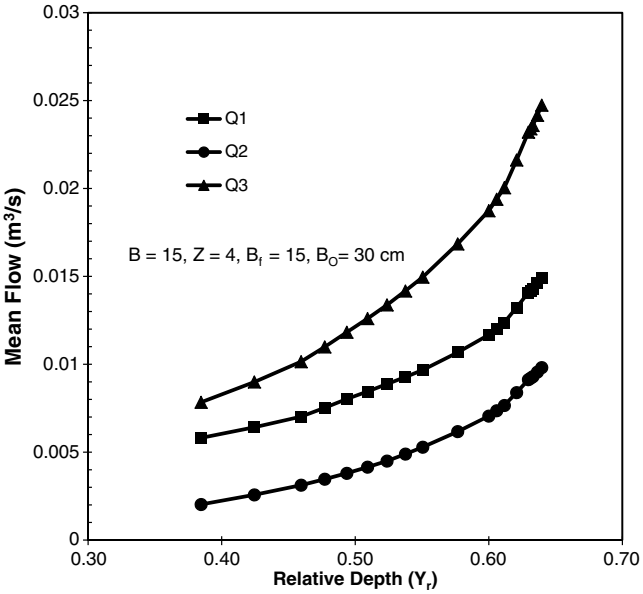

Fig. 7. Mean flow data for compound cross-section Type 5

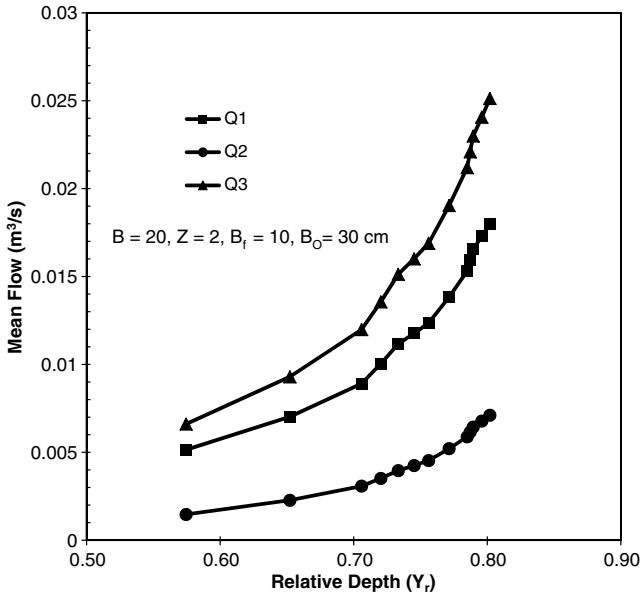

Fig. 9. Mean flow data for compound cross-section Type 7

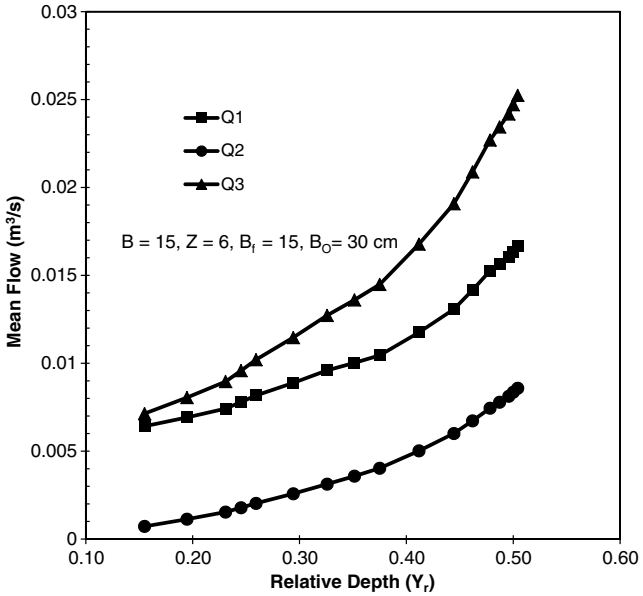

Fig. 8. Mean flow data for compound cross-section Type 6

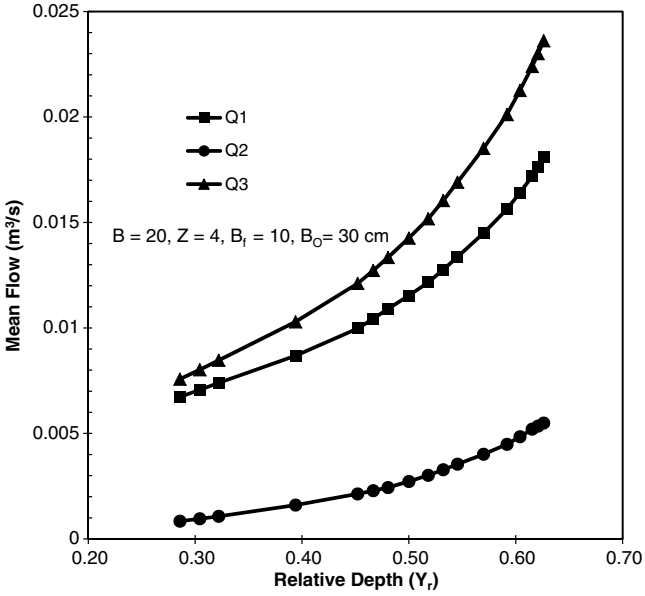

Fig. 10. Mean flow data for compound cross-section Type 8

30 cm flume width (i.e., first set of models). Relative depth is defined as the ratio of the depth above floodplain bed (Y_f) to the total depth associated with the compound cross section (h). Figs. 3–11 depict the general trend of the interaction mechanism between the three types of mean volumetric flow rate for the nine tested models of different geometry.

Figs. 3–11 show the mean volumetric flow rate in the total asymmetric compound cross section (Q_3) to be approximately equal to the sum of the mean volumetric flow rate in the main channel (Q_1) and the mean volumetric flow rate in the floodplain (Q_2). For all models presented in Figs. 3–11, the three volumetric flow rates consistently increase with the increase in the relative depth (Y_r). In addition, Figs. 3–5 show that the volumetric flow rate in the main channel (Q_1) to be higher than the volumetric flow rate in the floodplain (Q_2) considering the lower range of Y_r values; however, this trend is reversed at a critical value of Y_r. This reversed trend can only happen for models associated with a main channel width (B) that is smaller than the floodplain width (B_f). Figs. 3–5 show the critical value of Y_r is inversely proportional to the step height (Z). For example, Fig. 3 is associated with 0.57 critical Y_r value and 2 cm step height compared with Fig. 4, which is associated with 0.48 critical Y_r value and 4 cm step height. Figs. 6–11 represent models with a main channel width (B) that is equal to or greater than the floodplain width (B_f), which results in the main channel volumetric flow rate being consistently larger than the floodplain volumetric flow rate. The former observations as concluded from Figs. 3–11 are consistent with the normal expectations related to open-channel flow.

Single-Variable Regression Prediction Models

A generalized single-variable regression model has been derived to predict each of the three experimentally measured mean volumetric

J. Irrig. Drain Eng. 2013.139:542-550.

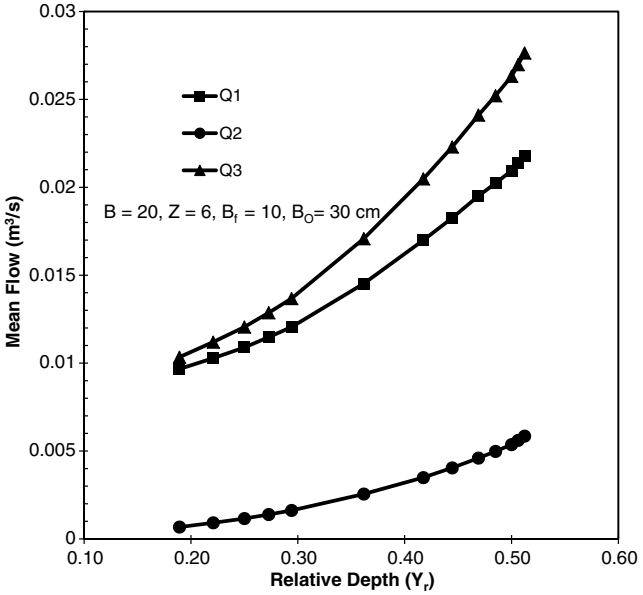

Fig. 11. Mean flow data for compound cross-section Type 9

flow rates as a function of relative depth (Y_r). The prediction model is exponential in form as indicated by Eq. (3). The linear multiple-variable regression techniques will be used to estimate the regression coefficients associated with the model after performing the necessary linear transformation

$$\mathrm{Ln}(Q_{i,j}) = a + bY_r + cY_r^n \tag{3}$$

where Ln = natural logarithm function; $Q_{i,j}$ = the ith mean volumetric flow-rate type associated with the jth compound cross-section type ($i = 1, 2, 3$; $j = 1, 2, \ldots, 9$); a = regression constant; b, c = regression coefficients associated with independent variables Y_r, Y_r^n, respectively; n = regression power for independent variable Y_r in the non-linear term; and Y_r = independent variable representing relative depth.

Table 3 provides the derived numerical values of the regression parameters (a, b, c, n) for a total of 27 different models representing three types of mean volumetric flow rate for each of the nine different asymmetric compound cross-section cases considered by the first set of models. When deriving the generalized model provided in Eq. (3), optimization of the three main regression statistics was done to arrive at the best possible estimated regression equation. The first main statistic is the standard error ($S_{Qi,j}$) associated with the dependent variable ($Q_{i,j}$), which has been minimized to the lowest possible values as provided in Table 4. The second main statistic is the model coefficient of determination (R^2), which has been maximized to very high values ranging from 0.988 to 0.999. The third main statistic is the Student's t-value associated with the independent variable coefficients (b and c), which have been maximized to reflect high significance with a confidence level ranging from 97.5 to 99.9%.

In addition to the preceding three main statistics, the normal probability plots and residual plots are produced for each regression model to test the assumptions of normality and constant variance of the error terms; and whenever a deviation from these assumptions was found, a modification of the model was sought. Table 4 also provides for each model the coefficient of variation for the dependent variable ($Q_{i,j}$) with the corresponding values being less than 1% for 25 out of 27 total cases. The coefficient of variation ($\mathrm{CV}_{i,j}$) is defined as the ratio of the standard error ($S_{Qi,j}$) to the mean volumetric flow-rate value ($\bar{Q}_{i,j}$) in a percentage.

All obtained statistics indicate that the derived regression models fit the data very well and that they have a very high predictive ability. Therefore, the derived general exponential model presented in Eq. (3) is a reliable and effective model to be used in estimating mean volumetric flow rates in open channels of asymmetrical rectangular compound cross sections. The model regression parameters (a, b, c, n) need to be estimated for any particular cross-section geometry because Table 3 indicates that these coefficients are different for each compound cross-section type.

The single-variable regression models associated with the second set of prototype models (six cases) are of the same form as presented in Eq. (3), and the corresponding statistics indicate that they are as significant as those associated with the first set of models. However, the results are not presented in this paper because of space limitations; in lieu, the multiple-variable regression models for both sets of prototype models will be presented in the next section.

Multiple-Variable Regression Prediction Models

A generalized multiple-variable regression model has been derived to predict each of the three experimentally measured mean volumetric flow rates as a function of three dimensionless parameters. The first dimensionless parameter is the relative depth (Y_r) used as the main parameter in developing the single-variable regression models. The two additional dimensionless parameters take into consideration the channel width dimensions (B_f, B) and step height (Z). The prediction model is also exponential in form as indicated by the following:

Table 3. Regression Coefficients for Single-Variable Prediction Models

Flow type (i)	Regression parameters	Compound cross-section type (j)								
		1	2	3	4	5	6	7	8	9
Q_1	a	−2.183	−6.422	−5.626	−1.043	−5.029	−5.228	−2.987	−5.254	−5.038
	b	−15.01	0.997	−0.127	−16.48	−2.607	0.785	−10.72	0.063	1.848
	c	14.655	2.558	4.120	15.390	6.038	2.865	11.753	3.043	1.027
	n	2	2	2	2	2	2	2	2	2
Q_2	a	−4.289	−8.113	−7.612	−4.174	−7.498	−8.793	−4.978	−8.603	−9.155
	b	−9.467	5.740	5.863	−10.29	1.885	11.692	−9.493	5.420	11.224
	c	11.830	0	0.297	12.211	4.025	−7.452	11.875	0	−6.720
	n	2	1	2	2	2	2	2	1	2
Q_3	a	−2.631	−6.951	−5.661	−1.524	−5.030	−5.328	−2.830	−5.271	−5.077
	b	−12.07	4.789	1.762	−14.30	−1.818	2.251	−10.68	0.554	2.434
	c	13.228	0	3.360	14.338	6.046	1.984	11.983	2.984	0.924
	n	2	1	2	2	2	2	2	2	2

J. Irrig. Drain Eng. 2013.139:542-550.

Table 4. Regression Statistics for Single-Variable Prediction Models

Flow type (i)	Regression parameters	Compound cross-section type (j)								
		1	2	3	4	5	6	7	8	9
Q_1	$S_{Qi,j}$	0.0248	0.0144	0.0208	0.0091	0.0177	0.0182	0.0203	0.0071	0.0098
	R^2	0.997	0.999	0.996	0.999	0.997	0.997	0.998	0.999	0.999
	t_b	−8.215	1.402	−0.231	−14.23	−3.274	2.594	−6.056	0.420	7.940
	t_c	11.570	3.884	6.313	19.517	8.051	6.633	9.297	18.865	3.198
	$CV_{i,j}$	0.48%	0.28%	0.41%	0.18%	0.35%	0.36%	0.40%	0.14%	0.19%
Q_2	$S_{Qi,j}$	0.0227	0.0143	0.0208	0.0109	0.0207	0.0423	0.0245	0.0145	0.0178
	R^2	0.998	0.999	0.999	0.999	0.998	0.997	0.998	0.999	0.999
	t_b	−5.646	131.44	10.637	−7.449	2.026	16.580	−4.860	168.45	26.508
	t_c	10.176	NA	0.455	12.965	4.592	−7.402	8.480	NA	−11.51
	$CV_{i,j}$	0.49%	0.31%	0.45%	0.23%	0.44%	0.90%	0.52%	0.31%	0.38%
Q_3	$S_{Qi,j}$	0.0232	0.0159	0.0203	0.0098	0.0181	0.0179	0.0207	0.0072	0.0089
	R^2	0.998	0.999	0.998	0.999	0.998	0.998	0.998	0.999	0.999
	t_b	−7.055	98.056	3.281	−11.50	−2.232	7.557	−5.935	3.642	11.435
	t_c	11.149	NA	5.274	16.935	7.877	4.666	9.286	18.178	3.146
	$CV_{i,j}$	0.56%	0.38%	0.49%	0.23%	0.43%	0.43%	0.50%	0.17%	0.21%
Sample size		21	13	19	17	19	17	13	17	13

Note: NA = Not applicable because the corresponding coefficient value is zero.

$$\mathrm{Ln}(Q_i) = a_1 + b_1 B_1 + b_2 B_1^2 + c_1 B_2 + c_2 B_2^4 + d_1 Y_r + d_2 B_2^{n_1} Y_r^{n_2} \quad (4)$$

where $B_1 = (B_f/Z)$; $B_2 = (B_f/B)$; $Y_r = (Y_f/h)$; $Z = (h - Y_f)$; Ln = natural logarithm function; Q_i = the ith mean volumetric flow-rate type ($i = 1, 2, 3$) in m^3/s; a_1 = regression constant; b_1, b_2, c_1, c_2, d_1, and d_2 = regression coefficients; and n_1 and n_2 = regression powers associated with independent variables B_2 and Y_r, respectively.

According to Eq. (4), a multiple-variable predictive model can be derived for each mean volumetric flow-rate type resulting in three different regression models. Therefore, the volumetric flow-rate measurements estimated for a particular mean volumetric flow-rate type as obtained from the nine different compound cross-section types (i.e., first set of models) will be pooled together for the purpose of developing one multiple-variable regression model for each mean volumetric flow-rate type. Although the relationship between the dependent variable and the independent variables in Eq. (4) is a nonlinear one, the equation is linear in terms of the coefficients and, hence, the linear multiple-variable regression techniques can be applied, which are mainly dependent on the minimization of the sum of squared errors.

Table 5 provides the derived regression parameters (a_1, b_1, b_2, c_1, c_2, d_1, and d_2) and corresponding statistics for the three mean volumetric flow-rate types considering the first set of models with 30 cm flume width. Table 6 provides the same regression parameters and statistics but for the second set of models with 60 cm flume width. The regression parameters are relatively close to each other in magnitude when compared with the regression parameters obtained for the single variable regression models. The adjusted R^2 has ranged from 0.970 to 0.985, which means that 97.0 to 98.5% of the variation in the mean volumetric flow rate is explained by the variations in the three dimensionless parameters (B_1, B_2, and Y_r). However, the adjusted R^2 for the second set of models has ranged from 0.985 to 0.988 as provided in Table 6. These R^2 values are considered very high but slightly smaller than those associated with the derived single-variable regression models. This can be attributed to the more homogeneity of the data used to develop the single-variable models compared with the data used in the multiple-variable models.

The same notice and explanation apply to the second primary statistic, namely, the coefficients of variation wherein their values

Table 5. Regression Coefficients and Statistics for Multiple-Variable Prediction Models Using 30-cm Flume Width

Statistics	Q_1	Q_2	Q_3
R^2	0.973	0.986	0.972
R^2_{adj}	0.971	0.985	0.970
S_{Qi}	0.0780	0.0844	0.0727
COV_i (%)	1.52	1.81	1.74
n_1	0.4	0.4	0.4
n_2	2.7	2.7	2.7
a_1	−5.369	−5.427	−4.914
b_1	−0.358	−0.395	−0.370
b_2	0.024	0.033	0.028
c_1	0	1.185	0.305
c_2	−0.609	−1.536	−0.694
d_1	1.459	5.391	2.108
d_2	2.395	0.960	2.544
t_{b1}	−41.427	−42.323	−46.068
t_{b2}	12.996	16.498	16.08
t_{c1}	NA	41.541	12.414
t_{c2}	−8.759	−20.453	−10.727
t_{d1}	7.927	27.091	12.294
t_{d2}	13.469	4.993	15.354

Note: NA = Not applicable since the corresponding coefficient value is zero.

are higher in the multiple-variable regression models compared with the values associated with the single-variable models; however, they are still acceptably small with values below 1.81% (1.52–1.81%) considering the first set of models (Table 5). However, the corresponding values for the second set of models are slightly larger ranging from 2.43 to 2.71% as provided in Table 6. The third primary statistic is the Student's t-value associated with the independent variable coefficients (b_1, b_2, c_1, c_2, d_1, and d_2). The corresponding t-values have been maximized to reflect high significance with a confidence level higher than 99% for both sets of models.

In addition to the aforementioned three main statistics, normal probability plots and residual plots have been obtained for the three multiple-regression models. These plots showed that there were no deviations from the assumptions of linearity, normality, and constant variance for the error terms associated with the derived predictive models. Hence, it can be concluded that the regression

J. Irrig. Drain Eng. 2013.139:542-550.

Table 6. Regression Coefficients and Statistics for Multiple-Variable Prediction Models Using 60-cm Flume Width

Statistic	Q_1	Q_2	Q_3
R^2	0.988	0.987	0.989
R^2_{adj}	0.986	0.985	0.988
S_{Qi}	0.0834	0.1489	0.0833
COV_i (%)	2.43	3.18	2.71
n_1	0.4	0.4	0.4
n_2	2.7	2.7	2.7
a_1	−3.793	−4.221	−3.515
b_1	−0.331	−0.345	−0.339
b_2	0.028	0.038	0.032
c_1	0	1.156	0.237
c_2	−0.336	−0.863	−0.365
d_1	2.361	7.970	2.856
d_2	1.818	−0.735	2.188
t_{b1}	−39.554	−23.119	−40.654
t_{b2}	9.214	7.158	10.808
t_{c1}	NA	27.103	9.929
t_{c2}	−8.595	−12.355	−9.351
t_{d1}	12.134	22.946	14.705
t_{d2}	8.306	−1.881	10.015

Note: NA = Not applicable since the corresponding coefficient value is zero.

Table 7. MSE and MSPR Associated with the Three Multiple-Variable Regression Models

Dependent variable	Flume width ($B_O = 30$ cm)		Flume width ($B_O = 60$ cm)	
	MSE	MSPR	MSE	MSPR
Ln Q_1	0.00609	0.00885	0.00695	0.00836
Ln Q_2	0.00711	0.01013	0.02217	0.02908
Ln Q_3	0.00529	0.00580	0.00692	0.00866

models developed for the three mean volumetric flow rates fit the data very well. Finally, the generated regression models were validated using a holdout sample of approximately 40% of the total sample size (i.e., 60 observed volumetric flow-rate measurements) to verify the models' predictive strength. The corresponding mean of the squared prediction errors (MSPR) was calculated for each mean volumetric flow rate considering the two sets of models (i.e., $B_O = 30$ and 60 cm) with the results provided in Table 7. Table 7 clearly shows that the MSPR values associated with both sets of models, as obtained from Eq. (5), are close to their corresponding mean squared errors (MSE). This means that the MSE statistic was not seriously biased, and it provided an appropriate indication of the predictive ability of the derived multiple-variable regression models (Kutner et al. 2005).

$$\text{MSPR} = \frac{\sum_{i=1}^{n^*}(Y_i - \hat{Y}_i)^2}{n^*} \tag{5}$$

where Y_i = the value of the response variable in the ith validation case; $\hat{Y}_i$ = the predicted value of the response variable for the ith validation case based on the model-building data set; and n^* = the number of cases in the validation data set (60 cases).

An effort was made to develop one set of multiple-variable regression models that deploys the experimental results obtained from the two sets of models with different flume width. However, the relevant statistics were relatively weak; therefore, a separate set of multiple-variable regression models was developed for models with 30 and 60 cm flume widths. The developed regression models are only applicable to conditions similar to those used in the experimental work.

Conclusions

Experimental results of mean volumetric flow-rate measurements have been presented for the first set of models consisting of nine different models constructed using an asymmetric rectangular compound channel configuration. The variations and interactions of three mean volumetric flow rates, namely, those associated with the floodplain, main-channel, and full channel cross section, have been investigated in relationship to a single dimensionless parameter named relative depth. The first three channel configurations associated with a main channel width smaller than the floodplain width have resulted in the main channel mean volumetric flow rate to be higher than the floodplain mean volumetric flow rate, provided the relative depth is smaller than a corresponding critical value. The critical relative depth value is different for each investigated model, and it is inversely proportional to the step height. The remaining six channel configurations associated with a main channel width equal to or greater than the floodplain width have caused the main channel mean volumetric flow rate to be consistently higher than the floodplain mean volumetric flow rate.

A total of 27 single-variable regression models have been developed for the three mean volumetric flow rates considering the first set of models comprising nine different compound cross-section configurations. The predictive models developed are exponential in form and primarily use the relative depth as the main dependent variable. The statistical reliability of the derived models was investigated using three primary statistics, namely, the model standard error, model coefficient of determination, and Student's t-value. The corresponding statistics' values are very high, indicating the very high significance of the derived predictive models. Also, the normal probability plots and residual plots were developed and examined for the 27 predictive models, concluding that these models fit the data very well and the assumptions of normality and constant variance for the error term are very well valid.

The mean volumetric flow-rate measurements for the first set of compound cross-section configurations were pooled together for the purpose of generating a multiple-variable regression model for each mean volumetric flow-rate type. The result is three distinct multiple-variable predictive models, which are function of three dimensionless dependent parameters. The three dimensionless parameters include the channel relative depth and two other dimensionless parameters defined in terms of the channel width dimensions. A similar set of multiple-variable predictive models have developed for the second set of asymmetric compound cross-section configurations. The same three primary statistics outlined earlier have indicated the high reliability and significance of the derived multivariable predictive models. Additional model validation was done including the normal probability plots, residual plots, and mean of the squared prediction errors (MSPR). These validation measures have all indicated the appropriateness of the derived models in predicting the three mean volumetric flow-rate types.

Notation

The following symbols are used in this paper:

A = cross sectional flow area of the channel;
a, a_1 = regression constants;
B = bottom width of the main channel;
B_f = floodplain channel width;
B_O = bottom width of the upstream channel;

J. Irrig. Drain Eng. 2013.139:542-550.

B_1 = (B_f/Z);
B_2 = (B_f/B);
b, c = regression coefficients associated with independent variables Y_r, Y_r^n respectively;
b_1, b_2, c_1, c_2, d_1, and, d_2 = regression coefficients;
h = main channel water depth;
Ln = natural logarithm function;
N = number of small differential areas;
n = regression power for independent variable Y_r in the nonlinear term;
n_1 and n_2 = regression powers associated with independent variables B_2 and Y_r, respectively;
n^* = the number of cases in the validation data set;
Q = cross sectional mean volumetric flow rate;
Q_i = ith mean volumetric flow-rate type ($i = 1, 2, 3$) in m^3/s;
Q_{ij} = the ith mean volumetric flow-rate type associated with the jth compound cross-section type;
Q_1 = mean main channel volumetric flow rate;
Q_2 = mean floodplain volumetric flow rate;
Q_3 = mean full cross sectional volumetric flow rate;
R^2 = coefficient of determination;
S_{Qij} = standard error associated with the mean volumetric flow rate (Q_{ij});
t = Student's t-value statistic;
u_i = measured point velocity;
Y_f = floodplain water depth;
Y_i = the value of the response variable in the ith validation case;
Y_r = independent variable representing relative depth = Y_f/h;
$\hat{Y}_i$ = the predicted value for the ith validation case based on the model-building data set;
Z = step height;
ΔA_i = small differential areas ($I = 1, 2, \ldots, N$); and
θ_1 and θ_2 = enterance angles.

References

Ackers, P. (1992). "Hydraulic design of two-stage channels." *Proc. ICE–Water Marit. Energy*, 96(4), 247–257.

Ackers, P. (1993). "Flow formulae for straight two-stage channels." *J. Hydraul. Res.*, 31(4), 509–531.

Anderson, M. G., Walling, D. E., and Bates, P. D. (1996). *Floodplain processes*, Wiley, New York.

Atabay, S., Knight, D. W., and Seckin, G. (2005). "Effects of overbank flow on fluvial sediment transport rates." *Proc. ICE–Water Manage.*, 158(1), 25–34.

Babaeyan-Koopai, K., Ervine, D. A., Carling, P. A., and Cao, Z. (2002). "Velocity and turbulence measurements for two overbank flow events in River Severn." *J. Hydraul. Eng.*, 128(10), 697–705.

Bousmar, D., Wilkin, N., Jacquemart, J. H., and Zech, Y. (2004). "Overbank flow in symmetrically narrowing floodplains." *J. Hydraul. Eng.*, 130(4), 305–312.

Carollo, F. G., Ferro, V., and Termini, D. (2002). "Flow velocity measurements in vegetated channels." *J. Hydraul. Eng.*, 128(7), 669–673.

Ervine, D. A., Babaeyan-Koopai, K., and Sellin, R. H. J. (2000). "Two-dimensional solution for straight and meandering overbank flows." *J. Hydraul. Eng.*, 126(9), 653–669.

Hosseini, S. M. (2004). "Equations for discharge calculation in compound channels having homogeneous roughness." *Iran. J. Sci. Technol.*, 28(B5), 538–546.

Karamisheva, R., Lyness, J. F., Myers, W. R. C., and Cassells, J. B. (2005). "Improving sediment discharge prediction for overbank flows." *Proc. ICE–Water Manage.*, 158(1), 17–24.

Karamisheva, R. D., Lyness, J. F., Myers, W. R. C., Cassells, J. B. C., and O'Sullivan, J. (2006). "Overbank flow depth prediction in alluvial compound channels." *Proc. ICE–Water Manage.*, 159(3), 195–205.

Knight, D. W., et al. (1999). "The response of straight mobile bed channels to inbank and overbank flows." *Proc. ICE–Water, Marit., Energy*, 136(4), 211–224.

Knight, D. W., and Brown, F. A. (2001). "Resistance studies of overbank flow in rivers with sediment using the flood channel facility." *J. Hydraul. Res.*, 39(3), 283–301.

Knight, D. W., and Demetriou, J. D. (1983). "Floodplain and main channel flow interaction." *J. Hydraul. Eng.*, 109(8), 1073–1091.

Knight, D. W., and Hamed, M. E. (1984). "Boundary shear in symmetrical compound channel." *J. Hydraul. Eng.*, 110(10), 1412–1430.

Kutner, M., Nachtsheim, C., Neter, J., and Li, W. (2005). *Applied linear statistical models*, McGraw-Hill/Irwin, New York.

Lambert, M. F., and Myers, W. R. C. (1998). "Estimating the discharge capacity in straight compound channels." *Proc. ICE–Water, Marit., Energy*, 130(2), 84–94.

Maghrebi, M. F., and Ball, J. E. (2006). "New method for estimation of discharge." *J. Hydraul. Eng.*, 132(10), 1044–1051.

Myers, W. R. C., Knight, D. W., Lyness, J. F., Cassells, J. B., and Brown, E. (1999). "Resistance coefficient for inbank and overbank flows." *Proc. ICE–Water, Marit., Energy*, 136(2), 105–115.

Myers, W. R. C., Lyness, J. F., Cassells, J. B., and O'Sullivan, J. J. (2000). "Geometrical and roughness effects on compound channel resistance." *Proc. ICE–Water Marit. Energy*, 142(3), 157–166.

Rezaei, B., and Knight, D. W. (2011). "Overbank flow in compound channels with nonprismatic floodplains." *J. Hydraul. Eng.*, 137(8), 815–824.

Shiono, K., Al-Romaih, J. S., and Knight, D. W. (1999). "Stage-discharge assessment in compound meandering channels." *J. Hydraul. Eng.*, 125(1), 66–77.

Wormleaton, P. R., Allen, J., and Hadjipanos, P. (1982). "Discharge assessment in compound channel flow." *J. Hydraul. Div.*, 108(9), 975–993.

J. Irrig. Drain Eng. 2013.139:542-550.